JACS
JOURNAL OF THE AMERICAN CHEMICAL SOCIETY
pubs.acs.org/JACS
Article

# Fabrication of Two-Dimensional Platelets with Heat-Resistant Luminescence and Large Two-Photon Absorption Cross Sections via Cooperative Solution/Solid Self-Assembly

Yanjun Gong,[⊥] Liyang Fu,[⊥] Yanxue Che, Hongwei Ji, Yifan Zhang,* Ling Zang, Jincai Zhao, and Yanke Che*

Cite This: J. Am. Chem. Soc. 2023, 145, 9771−9776
Read Online



**ABSTRACT:** The combination of solution self-assembly, which enables primary morphological control, and solid self-assembly, which enables the creation of novel properties, can lead to the formation of new functional materials that cannot be obtained using either technique alone. Herein, we report a cooperative solution/solid self-assembly strategy to fabricate novel two-dimensional (2D) platelets. Precursor 2D platelets with preorganized packing structure, shape, and size are formed via the living self-assembly of a donor−acceptor fluorophore and volatile coformer (i.e., propanol) in solution phase. After high-temperature annealing, propanol is released from the precursor platelets, and new continuous intermolecular hydrogen bonds are formed. The new 2D platelets formed retain the controllable morphologies originally defined by the solution phase living self-assembly but exhibit remarkable heat-resistant luminescence up to 200 °C and high two-photon absorption cross sections (i.e., >19,000 GM at 760 nm laser excitation).

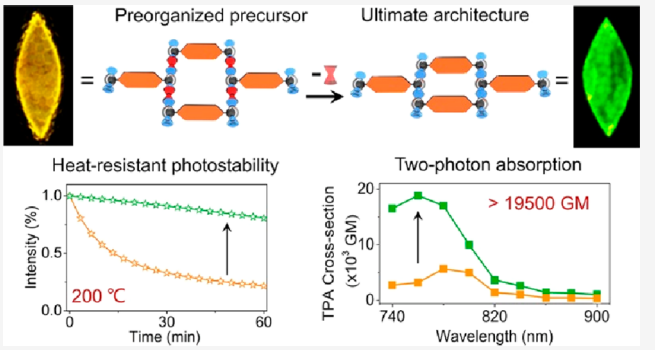


## INTRODUCTION

Solution self-assembly has been widely used to fabricate ordered functional materials from polymers and small-molecule building blocks.[1−5] In particular, living self-assembly provides an unprecedented level of control over molecular organization, enabling the development of a wide range of complex one-[6−16] and two-dimensional (2D)[17−20] architectures from single or multiple components. Solvents play a key role in the solution self-assembly, not only controlling the assembly pathway[7−13,19] but also frequently acting as a supportive component in the resulting architectures.[15,16,20−22] However, the involvement of solvents may also have adverse effects, such as deactivating the pathways necessary for forming substantial structures and altering the intrinsic physical−chemical properties by acting as supportive components in the resulting assemblies.[20−22] To this regard, the solvent-free solid self-assembly can avoid the adverse effects of solvents and is thus advantageous for constructing supramolecular structures with pristine architectures.[23−27] Nevertheless, solid self-assembly presents an intrinsic challenge because the building blocks have limited mobility in solid state, making precise control over the long-range ordered structure very difficult. To date, only a few examples of the solvent-free self-assembly have been reported for constructing well-defined supramolecular structures.[23−25] To address this shortcoming and incorporate the advantages of solution self-assembly, we hypothesized that ordered architectures formed using solution self-assembly can serve as preorganized precursors for solid self-assembly. Precursors with preorganized molecular packing could greatly mitigate the need for molecular mobility in a solid self-assembly by providing considerably close molecular packing for transitioning into the final architecture.

To realize the above hypothesis, a volatile coformer was introduced to noncovalently bind the designed building blocks (i.e., organic fluorophores) in solution, self-assembling into well-defined shapes as the preorganized precursors. The volatile coformer was expected to be released from the crystals after annealing at an elevated temperature, allowing the generation of the freed monomeric building blocks from the binding by the coformer. Because the resulting individual building blocks are still adjacent to each other, self-assembly of them into a new architecture mode is thus facilitated in the solid state (Figure 1). In this study, we fabricated various 2D platelets via living self-assembly in solution, using donor−

Received: February 10, 2023
Published: April 20, 2023

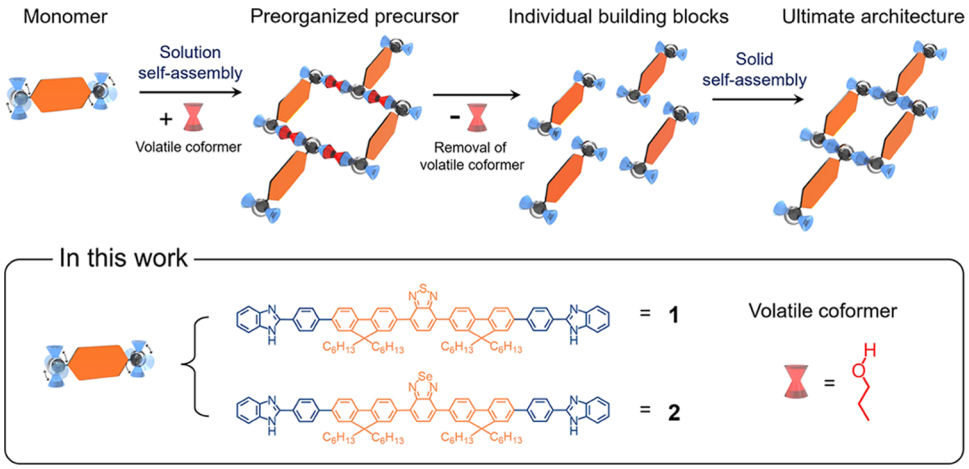


**Figure 1.** Schematic illustration of the cooperative solution/solid self-assembly strategy that creates a new architecture. D−A fluorophores **1** and **2** were used as the primary building blocks and 1-propanol as the volatile coformer.

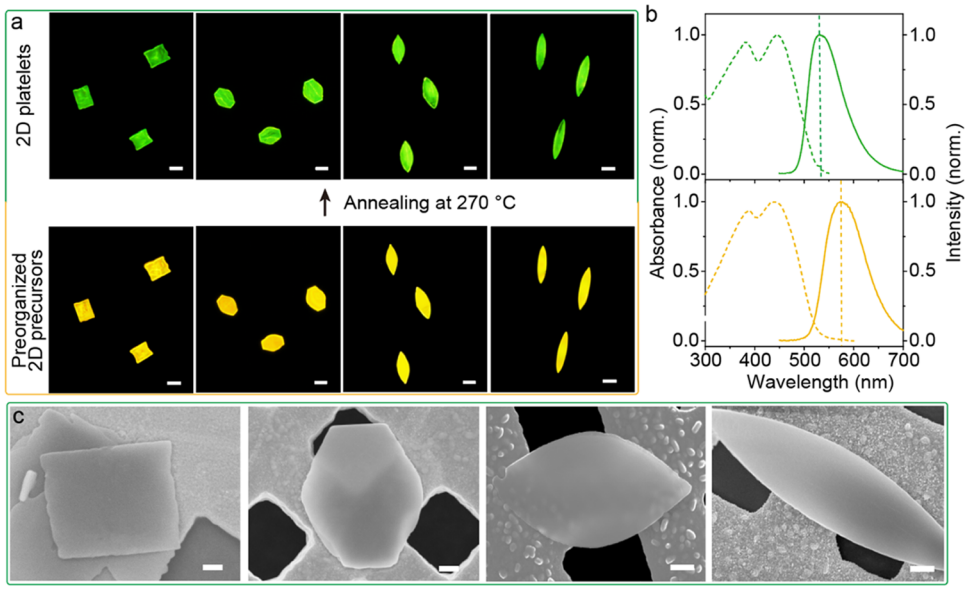


**Figure 2.** (a) Fluorescence-mode optical images and (b) UV−vis absorption (dashed) and fluorescence spectra (solid) of the preorganized 2D precursors (yellow) prepared from 1-propanol and **1** with four different shapes (rectangular, hexagonal, elliptic, and lorate) and the resulting 2D platelets (green) after annealing at 270 °C for 2 h. Scale bar: 10 $\mu$m. (c) SEM images of the resulting 2D platelets with four different shapes after annealing under the same condition. Scale bar: 2 $\mu$m.

acceptor (D−A) fluorophores as the primary building blocks and 1-propanol as the volatile coformer (Figure 1). These 2D platelets were selected because their shapes and sizes can be precisely controlled using a seeded living self-assembly method recently developed in our lab,[20] thereby providing rich morphologies for exploring the subsequent solid self-assembly. Extensive experiments demonstrated that after annealing at 270 °C, 1-propanol was released from the 2D platelets by breaking up the hydrogen bonds with the D−A fluorophores, and the freed D−A fluorophores were densely connected through new continuous intermolecular hydrogen bonds (Figure 1). Importantly, the resulting 2D platelets with the tightly packed D−A fluorophores exhibited considerably enhanced heat-resistant luminescence, for which the luminescence remained remarkably stable even at 200 °C.

Furthermore, the final 2D platelets exhibited large two-photon absorption (TPA) cross sections (e.g., >19,000 GM at an excitation wavelength of 760 nm), which were among the highest values reported for organic structures. In contrast, the precursor 2D platelets containing the coformer 1-propanol exhibited a sharp decline in luminescence at 200 °C and considerably lower TPA cross sections, highlighting the importance of fabrication of pure crystals with only primary building blocks. The cooperative solution/solid self-assembly strategy reported herein provides a new avenue to construct functional pure crystals that would otherwise be impossible to create using the solution or solid self-assembly methods alone.

## RESULTS AND DISCUSSION

**Solid Self-Assembly of Preorganized Precursors Fabricated from Solution Self-Assembly.** First, 2D precursors platelets with preorganized structure and varying shapes (e.g., rectangular, hexagonal, elliptic, and lorate) were fabricated from 1-propanol and D−A fluorophore **1** (Figure 1) using the previously reported living seeded self-assembly method.[20] The $^1$H NMR spectra of the precursors (Figure



https://doi.org/10.1021/jacs.3c01517
J. Am. Chem. Soc. 2023, 145, 9771−9776

S1) revealed the characteristic peaks of 1-propanol in the dissolved samples of the 2D precursors, confirming the presence of 1-propanol. The optical properties (Figure S2) of the 2D precursors resembled those previously formed from 1-hexanol and fluorophore **1**, indicative of the formation of the same continuous hydrogen bonds between alcohols and **1**. To determine if the preorganized 2D precursors with all four shapes could reorganize into new crystals under solvent-free conditions, the precursors were placed on copper grids and annealed at 270 °C for 2 h. The annealing caused the fluorescent emissions from the four precursors to change from yellow to green (Figure 2a), indicating that a new molecular packing had formed during the annealing process. The fluorescence spectra confirmed that a fluorescence blueshift from 580 to 538 nm occurred in the four precursors (Figure 2b). Given the high temperature of annealing, we believed that 1-propanol was released from the precursor 2D platelets and the freed neighboring monomers **1** underwent solid self-assembly into a new ordered structure. To support this hypothesis, we performed $^{1}$H NMR analysis of the annealed 2D platelets dissolved in *d*-tetrahydrofuran. As shown in Figure S3, no characteristic $^{1}$H NMR peaks of 1-propanol were observed, indicating that 1-propanol was released from the precursors upon annealing. Notably, the UV−vis absorption of the resulting green-emissive 2D platelets was extremely similar to that of the yellow-emissive preorganized 2D precursors (Figure 2b). This is typical of D−A molecules, i.e., polar solvents were shown to have a negligible effect on the absorption of D−A fluorophore **1**.[20] To investigate whether the release of 1-propanol and the subsequent solid self-assembly of **1** resulted in crystal collapse, a scanning electron microscopy (SEM) analysis of the 2D platelets was conducted after annealing. Figure 2c shows that the surface of the resulting 2D platelets remained smooth, resembling that of the precursors (Figure S4). Likewise, the preorganized 2D precursors fabricated from fluorophore **2** and 1-propanol were capable of reorganizing into new crystals with the same shapes. Compared to **1**, fluorophore **2** has a stronger electronic acceptor (A) group (benzoselenadiazole), which produces a red emission of the 2D precursors, as shown in Figure S5, while the precursor of **1** yields a yellow emission (Figure 2a). Annealing of the 2D precursors of **2** at 285 °C for 2 h caused the fluorescent emission change from red to orange (Figure S5), indicating the same solid self-assembly of molecular packing as observed for fluorophore **1**. The results obtained for both **1** and **2** demonstrate the extensibility of the cooperative solution/solid self-assembly strategy that may be applicable to different building blocks.

To highlight the role of the volatile coformer (1-propanol), which enabled the organized structure to form the final architecture, we fabricated rod crystals from **1** without 1-propanol using convenient self-assembly in solution and used them as preorganized precursors for solid self-assembly under the same annealing conditions. Figure S6 shows that no new crystal structure formed, likely because no hydrogen bonds were formed to generate a necessary preorganized structure (Figure S7). This further emphasizes the key role of the volatile coformer in bringing the fluorophores to the proximity required for solid self-assembly.

**Crystal Structure of the Green-Emissive 2D Platelets from 1.** Careful examination of a typical green-emissive 2D platelet under fluorescent-mode optical microscopy revealed that its length (the *a*-axis) decreased from 28.3 to 24.1 $\mu$m and the width (the *c*-axis) increased from 9.4 to 10.1 $\mu$m after annealing (Figure 3a). This observation indicated that the solid

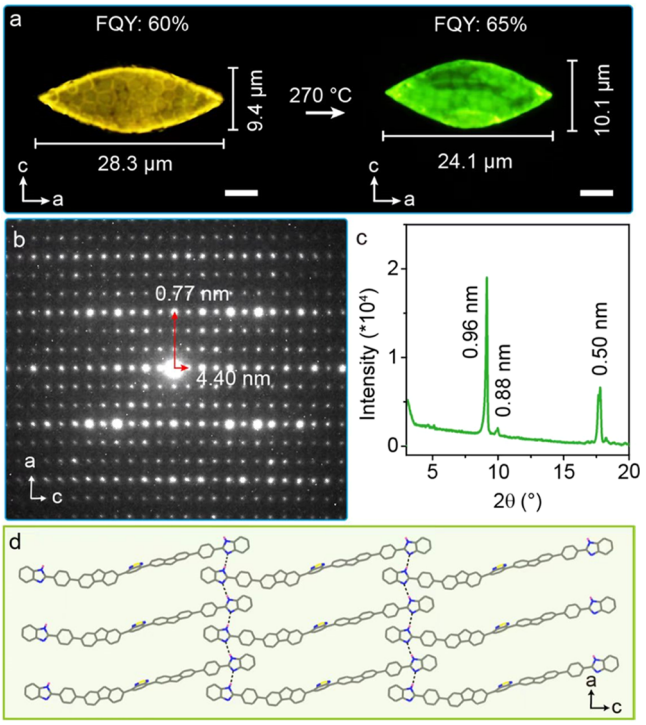


**Figure 3.** (a) Fluorescent-mode optical microscopic images of a typical yellow-emissive 2D precursor and the resulting green-emissive 2D platelet after annealing. Scale bar: 10 $\mu$m. Note: the texture of copper grid is clearly revealed underneath the thin platelet. (b) SAED patterns and (c) XRD spectrum of a green-emissive 2D platelet. (d) Simulated molecular packing within the green-emissive 2D platelet, which revealed new continuous hydrogen bonds along the *a*-axis.

self-assembly predominantly occurred along the *a*-axis, where the intermolecular distances were reduced. The infrared (IR) absorption spectrum of the green-emissive 2D platelets showed prominent absorption peaks at 3006, 3030, and 3063 cm$^{-1}$ (Figure S7), which are characteristic of intermolecular hydrogen bonds between the benzimidazole groups.[28] Based on these results, we conclude that new hydrogen bonds were formed between neighboring fluorophores **1** after the release of 1-propanol, causing the aforementioned size changes. Although this process did not result in crystal collapse in the small 2D platelets (Figure 2c), it caused some degree of destruction in the bulky crystals, rendering them unsuitable for single-crystal analysis. To gain detailed information on the molecular packing of **1**, selected area electron diffraction (SAED) and powder X-ray diffraction (XRD) measurements were conducted. The spot diffraction patterns of the green-emissive 2D platelets resembled those of the original precursors (Figure S8), indicating that the resulting green-emissive 2D platelets belonged to the same triclinic system with the space group P1. Notably, the SAED diffraction spots obtained on the green-emissive 2D platelets were remarkably extended in a large area (Figure 3b), indicating an enlarged coherent domain of fluorophore **1**. By combining the d-spacing values obtained on SAED (Figure 3b) with the XRD data (Figure 3c), the molecular packing in the green-emissive 2D platelets was simulated as shown in Figures 3d and S9, demonstrating that building blocks of **1** were connected via continuous


https://doi.org/10.1021/jacs.3c01517
J. Am. Chem. Soc. 2023, 145, 9771−9776

intermolecular hydrogen bonds. The new molecular connection can effectively explain the aforementioned size changes that occurred after annealing (Figure 3a).

**Heat-Resistant Luminescence of the Green-Emissive 2D Platelets.** Because the solid self-assembly into the green-emissive 2D platelets occurred at a high temperature, the resulting molecular packing was expected to be naturally resistant to heat, thereby exhibiting excellent heat-resistant luminescence. The fluorescence intensity (FL) of the green-emissive 2D platelets decreased extremely slowly at elevated temperatures (50, 100, and 200 °C) (Figure 4a), i.e., its

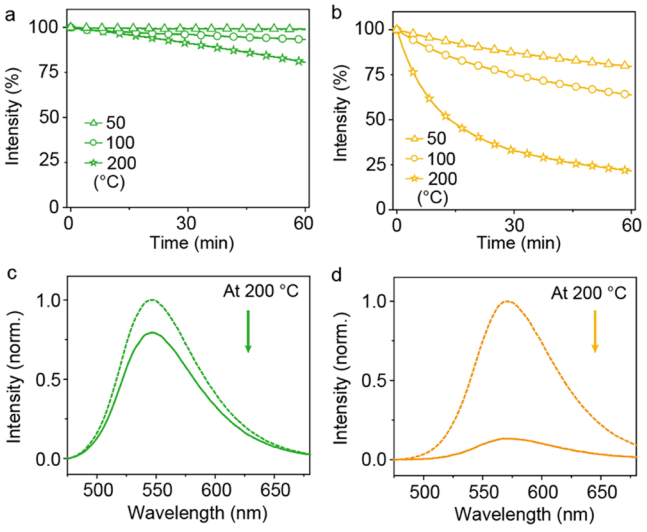


**Figure 4.** Fluorescence intensities of (a) green-emissive 2D platelets and (b) yellow-emissive precursors as a function of UV irradiation time (385 nm, 5 mW/cm$^2$) performed at different temperatures (50, 100, and 200 °C) in air. The fluorescence intensities were recorded in the range of 500−600 nm. Fluorescence spectra of (c) green-emissive 2D platelets and (d) yellow-emissive precursors before (dashed) and after (solid) 1 h of UV irradiation (385 nm, 5 mW/cm$^2$) at 200 °C.

fluorescence intensity decreased only by ∼20% at 200 °C after 1 h of UV irradiation (385 nm, 5 mW/cm$^2$) in air.[29] In contrast, the fluorescence intensity of the yellow-emissive precursors decreased rapidly (∼76%) under the same testing conditions (Figure 4b).[29] The distinct differences between the heat-resistant luminescence of the two platelets were also reflected by the differences in their fluorescence spectra at 200°C (Figure 4c,d).

The greater heat-resistant luminescence of the green-emissive 2D platelets can be correlated with the continuous intermolecular hydrogen bonds between building blocks **1**, which provide more effective protection of the active hydrogen atom in the benzimidazole unit from photo-oxidation[30] than the hydrogen bonds formed between **1** and the coformer (1-propanol) in the yellow-emissive precursors. This conclusion is further supported by the observation that the fluorescence intensity of rod crystals containing no hydrogen bonds (Figures S7 and S12), either between the benzimidazole units of **1** or between **1** and 1-propanol (fabrication details provided in the Supporting Information), decreased much faster than that of the preorganized 2D precursors under identical conditions (Figure S13). Therefore, the formation of continuous intermolecular hydrogen bonds serves as a new method for fabricating heat-resistant organic materials. The heat-resistant luminescence and high fluorescence quantum yield (FQY, 66%, as determined using integrated sphere technology) of the resulting 2D platelets will enable many applications in optoelectronics capable of operating under harsh environments.

**Large TPA Cross Sections of the Green-Emissive 2D Platelets.** In addition to improving the heat-resistant luminescence, the enlarged coherent domain of D−A fluorophore **1** owing to the continuous intermolecular hydrogen bonds and the enhanced crystal stability by thermal annealing are favorable for two-photon absorbing materials. Upon illumination by a femtosecond pulsed laser at 760 nm, the resulting 2D platelets and their precursors exhibit bright green and yellow emissions, respectively (Figure 5a,b),

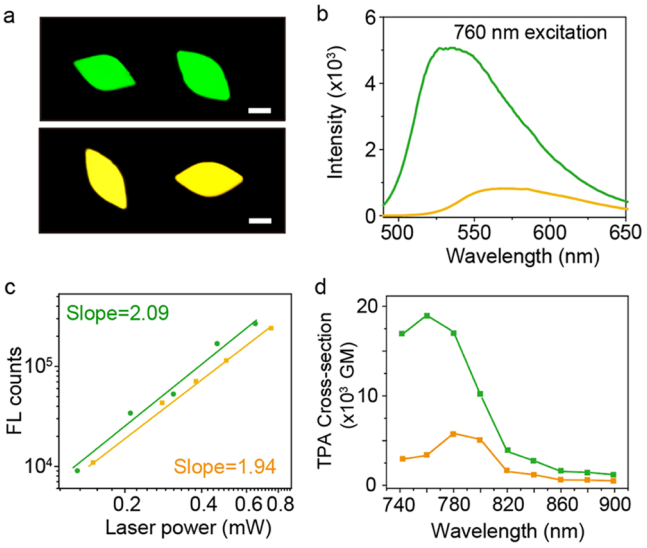


**Figure 5.** (a) Two-photon fluorescence microscopic images and (b) two-photon fluorescence spectra of the green-emissive 2D platelets (green) and their precursors (yellow) excited by a femtosecond pulsed laser at 760 nm. Scale bar: 10 $\mu$m. (c) Fluorescence intensity of the 2D platelets (green) and their precursors (yellow) as a function of femtosecond pulsed laser power (760 nm, 80 MHz, 140 fs pulsed duration). (d) TPA cross sections of the 2D platelets (green) and their precursors (yellow) at different excited wavelengths of a femtosecond pulsed laser (80 MHz, 140 fs pulsed duration).

indicative of a multiple-photon excitation process. Further, the linear relationship between the fluorescence intensity (FL) and the laser power (log(FL counts) vs log(excitation power)) produced a slope of 2.09 (Figure 5c), confirming a TPA process. Next, we measured the TPA cross sections of the green-emissive 2D platelets by applying laser excitation wavelengths from 740 to 900 nm. As shown in Figure 5d, the maximum TPA cross section of the green-emissive 2D platelets was ∼19,500 GM at an excitation wavelength of 760 nm, which is among the largest values reported for organic compounds (Table S1).[31−36] Notably, the maximum value of the TPA cross section of the green-emissive 2D platelets was ∼5 times that of the yellow-emissive precursors (Figure 5d), which were also capable of TPA (Figure 5c). This result highlights the importance of the continuous intermolecular hydrogen bonds in enhancing the optical properties; thus the resulting 2D platelets have a wide range of applications in the heat-resistant luminescence and two-photon fluorescence imaging.



https://doi.org/10.1021/jacs.3c01517
J. Am. Chem. Soc. 2023, 145, 9771−9776

## CONCLUSIONS

In conclusion, we have developed a cooperative solution/solid self-assembly strategy to fabricate new 2D platelets with heat-resistant luminescence and large TPA cross sections. Shape-controlled 2D platelets grown by living self-assembly of D−A fluorophores and volatile coformers are used as preorganized precursors. Thermal annealing of the precursors causes the release of volatile coformers, allowing the freed neighboring monomers to self-assemble into new 2D platelets while retaining the overall shapes. The continuous intermolecular hydrogen bonds formed between the building blocks by annealing at elevated temperatures offer excellent heat-resistant luminescence. Furthermore, this dense molecular packing greatly enhances the TPA cross sections of the 2D platelets compared with the precursors containing the volatile co-formers. The emerging novel optical properties and high emission efficiency of the 2D platelets with controlled geometry and size may lead to their broad applications in bioimaging and two-photon fluorescence imaging.

## ASSOCIATED CONTENT

### Supporting Information

The Supporting Information is available free of charge at https://pubs.acs.org/doi/10.1021/jacs.3c01517.

Synthesis details for fluorophores **1** and **2**, experimental details, property characterizations, crystal packing simulation details, TPA cross section calculations, and other supporting figures (PDF)

## AUTHOR INFORMATION


### Corresponding Authors

**Yifan Zhang** − *Key Laboratory of Photochemistry, CAS Research/Education Center for Excellence in Molecular Sciences, Institute of Chemistry, Chinese Academy of Sciences, Beijing 100190, China;* orcid.org/0000-0003-1298-5436; Email: yfzhang@iccas.ac.cn

**Yanke Che** − *Key Laboratory of Photochemistry, CAS Research/Education Center for Excellence in Molecular Sciences, Institute of Chemistry, Chinese Academy of Sciences, Beijing 100190, China; University of Chinese Academy of Sciences, Beijing 100049, China;* orcid.org/0000-0002-9671-3704; Email: ykche@iccas.ac.cn

### Authors

**Yanjun Gong** − *Key Laboratory of Photochemistry, CAS Research/Education Center for Excellence in Molecular Sciences, Institute of Chemistry, Chinese Academy of Sciences, Beijing 100190, China; University of Chinese Academy of Sciences, Beijing 100049, China*

**Liyang Fu** − *Key Laboratory of Photochemistry, CAS Research/Education Center for Excellence in Molecular Sciences, Institute of Chemistry, Chinese Academy of Sciences, Beijing 100190, China; University of Chinese Academy of Sciences, Beijing 100049, China*

**Yanxue Che** − *HT-NOVA Co., Ltd., Beijing 101312, China*

**Hongwei Ji** − *Key Laboratory of Photochemistry, CAS Research/Education Center for Excellence in Molecular Sciences, Institute of Chemistry, Chinese Academy of Sciences, Beijing 100190, China; University of Chinese Academy of Sciences, Beijing 100049, China*

**Ling Zang** − *Nano Institute of Utah, and Department of Materials Science and Engineering, University of Utah, Salt Lake City, Utah 84112, United States;* orcid.org/0000-0002-4299-0992

**Jincai Zhao** − *Key Laboratory of Photochemistry, CAS Research/Education Center for Excellence in Molecular Sciences, Institute of Chemistry, Chinese Academy of Sciences, Beijing 100190, China; University of Chinese Academy of Sciences, Beijing 100049, China;* orcid.org/0000-0003-1449-4235

Complete contact information is available at: https://pubs.acs.org/10.1021/jacs.3c01517

### Author Contributions

⊥Y.G. and L.F. contributed equally to this work.


### Notes

The authors declare no competing financial interest.

## ACKNOWLEDGMENTS

This work was funded by NSFC (nos. 21925604 and 22275196), National Key Research and Development Program of China (nos. 2019YFA0210401 and 2022YFA1206200), and the Strategic Priority Research Program of Chinese Academy of Sciences (grant no. XDB36000000).

## REFERENCES


(1) Whitesides, G. M.; Grzybowski, B. Self-Assembly at All Scales. *Science* **2002**, *295*, 2418−2421.

(2) MacFarlane, L. R.; Shaikh, H.; Garcia-Hernandez, J. D.; Vespa, M.; Fukui, T.; Manners, I. Functional nanoparticles through π-conjugated polymer self-assembly. *Nat. Rev. Mater.* **2021**, *6*, 7−26.

(3) Sun, M.; Lee, M. Switchable Aromatic Nanopore Structures: Functions and Applications. *Acc. Chem. Res.* **2021**, *54*, 2959−2968.

(4) Aida, T.; Meijer, E. W.; Stupp, S. I. Functional Supramolecular Polymers. *Science* **2012**, *335*, 813−817.

(5) Lutz, J.-F.; Lehn, J.-M.; Meijer, E. W.; Matyjaszewski, K. From precision polymers to complex materials and systems. *Nat. Rev. Mater.* **2016**, *1*, 16024.

(6) Jin, X. H.; Price, M. B.; Finnegan, J. R.; Boott, C. E.; Richter, J. M.; Rao, A.; Menke, S. M.; Friend, R. H.; Whittell, G. R.; Manners, I. Long-range exciton transport in conjugated polymer nanofibers prepared by seeded growth. *Science* **2018**, *360*, 897−900.

(7) Ogi, S.; Sugiyasu, K.; Manna, S.; Samitsu, S.; Takeuchi, M. Living supramolecular polymerization realized through a biomimetic approach. *Nat. Chem.* **2014**, *6*, 188−195.

(8) Choi, H.; Ogi, S.; Ando, N.; Yamaguchi, S. Dual Trapping of a Metastable Planarized Triarylborane π-System Based on Folding and Lewis Acid-Base Complexation for Seeded Polymerization. *J. Am. Chem. Soc.* **2021**, *143*, 2953−2961.

(9) Ogi, S.; Stepanenko, V.; Sugiyasu, K.; Takeuchi, M.; Wurthner, F. Mechanism of self-assembly process and seeded supramolecular polymerization of perylene bisimide organogelator. *J. Am. Chem. Soc.* **2015**, *137*, 3300−3307.

(10) Ślęczkowski, M. L.; Mabesoone, M. F. J.; Sleczkowski, P.; Palmans, A. R. A.; Meijer, E. W. Competition between chiral solvents and chiral monomers in the helical bias of supramolecular polymers. *Nat. Chem.* **2021**, *13*, 200−207.

(11) Liu, Y.; Peng, C.; Xiong, W.; Zhang, Y.; Gong, Y.; Che, Y.; Zhao, J. Two-Dimensional Seeded Self-Assembly of a Complex Hierarchical Perylene-Based Heterostructure. *Angew. Chem., Int. Ed.* **2017**, *56*, 11380−11384.

(12) Ma, X.; Zhang, Y.; Zhang, Y.; Liu, Y.; Che, Y.; Zhao, J. Fabrication of Chiral-Selective Nanotubular Heterojunctions through Living Supramolecular Polymerization. *Angew. Chem., Int. Ed.* **2016**, *55*, 9539−9543.

(13) Liu, Y.; Gong, Y.; Guo, Y.; Xiong, W.; Zhang, Y.; Zhao, J.; Che, Y.; Manners, I. Emergent Self-Assembly Pathways to Multidimen-

sional Hierarchical Assemblies using a Hetero-Seeding Approach. *Chem. - Eur. J.* **2019**, *25*, 13484−13490.
(14) Laishram, R.; Sarkar, S.; Seth, I.; Khatun, N.; Aswal, V. K.; Maitra, U.; George, S. J. Secondary Nucleation-Triggered Physical Cross-Links and Tunable Stiffness in Seeded Supramolecular Hydrogels. *J. Am. Chem. Soc.* **2022**, *144*, 11306−11315.
(15) Moreno-Alcántar, G.; Aliprandi, A.; Rouquette, R.; Pesce, L.; Wurst, K.; Perego, C.; Bruggeller, P.; Pavan, G. M.; De Cola, L. Solvent-Driven Supramolecular Wrapping of Self-Assembled Structures. *Angew. Chem., Int. Ed.* **2021**, *60*, 5407−5413.
(16) Zhang, Y.; Zhang, S.; Wu, H.; Dong, X.; Shi, P.; Qu, H.; Chen, Y.; Cao, X. Y.; Tian, Z. Q.; Hu, X.; Yang, L. Evolution of Transient Luminescent Assemblies Regulated by Trace Water in Organic Solvents. *J. Am. Chem. Soc.* **2022**, *144*, 19410−19416.
(17) Qiu, H.; Gao, Y.; Boott, C. E.; Gould, O. E. C.; Harniman, R. L.; Miles, M. J.; Webb, S. E. D.; Winnik, M. A.; Manners, I. Uniform patchy and hollow rectangular platelet micelles from crystallizable polymer blends. *Science* **2016**, *352*, 697−701.
(18) He, X.; Hsiao, M. S.; Boott, C. E.; Harniman, R. L.; Nazemi, A.; Li, X.; Winnik, M. A.; Manners, I. Two-dimensional assemblies from crystallizable homopolymers with charged termini. *Nat. Mater.* **2017**, *16*, 481−488.
(19) Fukui, T.; Kawai, S.; Fujinuma, S.; Matsushita, Y.; Yasuda, T.; Sakurai, T.; Seki, S.; Takeuchi, M.; Sugiyasu, K. Control over differentiation of a metastable supramolecular assembly in one and two dimensions. *Nat. Chem.* **2017**, *9*, 493−499.
(20) Gong, Y.; Cheng, C.; Ji, H.; Che, Y.; Zang, L.; Zhao, J.; Zhang, Y. Unprecedented Small Molecule-Based Uniform Two-Dimensional Platelets with Tailorable Shapes and Sizes. *J. Am. Chem. Soc.* **2022**, *144*, 15403−15410.
(21) Meng, W.; Kondo, S.; Ito, T.; Komatsu, K.; Pirillo, J.; Hijikata, Y.; Ikuhara, Y.; Aida, T.; Sato, H. An elastic metal-organic crystal with a densely catenated backbone. *Nature* **2021**, *598*, 298−303.
(22) Zhang, J.; Kosaka, W.; Sato, H.; Miyasaka, H. Magnet Creation by Guest Insertion into a Paramagnetic Charge-Flexible Layered Metal-Organic Framework. *J. Am. Chem. Soc.* **2021**, *143*, 7021−7031.
(23) Chen, Z.; Suzuki, Y.; Imayoshi, A.; Ji, X.; Rao, K. V.; Omata, Y.; Miyajima, D.; Sato, E.; Nihonyanagi, A.; Aida, T. Solvent-free autocatalytic supramolecular polymerization. *Nat. Mater.* **2022**, *21*, 253−261.
(24) Yano, K.; Itoh, Y.; Araoka, F.; Watanabe, G.; Hikima, T.; Aida, T. Nematic-to-columnar mesophase transition by in situ supramolecular polymerization. *Science* **2019**, *363*, 161−165.
(25) Xiong, H.; Zhou, H.; Sun, G.; Liu, Z.; Zhang, L.; Zhang, L.; Du, F.; Qiao, Z.-A.; Dai, S. Solvent-Free Self-Assembly for Scalable Preparation of Highly Crystalline Mesoporous Metal Oxides. *Angew. Chem., Int. Ed.* **2020**, *59*, 11053−11060.
(26) Zerkowski, J. A.; Seto, C. T.; Wierda, D. A.; Whitesides, G. M. Design of organic structures in the solid state: hydrogen-bonded molecular tapes. *J. Am. Chem. Soc.* **1990**, *112*, 9025−9026.
(27) Fouquey, C.; Lehn, J. M.; Levelut, A. M. Molecular recognition directed self-assembly of supramolecular liquid crystalline polymers from complementary chiral components. *Adv. Mater.* **1990**, *2*, 254−257.
(28) Fukaya, N.; Ogi, S.; Sotome, H.; Fujimoto, K. J.; Yanai, T.; Baumer, N.; Fernandez, G.; Miyasaka, H.; Yamaguchi, S. Impact of Hydrophobic/Hydrophilic Balance on Aggregation Pathways, Morphologies, and Excited-State Dynamics of Amphiphilic Diketopyrrolopyrrole Dyes in Aqueous Media. *J. Am. Chem. Soc.* **2022**, *144*, 22479−22492.
(29) Of note, the crystal structure of the green-emissive 2D platelets remained the same after 1 h of UV irradiation (385 nm, 5 mW/cm$^2$) at 200 °C in air, as evidenced by XRD results (Figure S10a). In contrast, the crystal structure of the yellow-emissive 2D platelets was demonstrated to undergo structural change under the same irradiation conditions (Figure S10b).
(30) The fluorescence intensity of the green-emissive 2D platelets decreased only by ∼3% after 1 h of UV irradiation (385 nm, 5 mW/cm$^2$) at 200 °C in argon (Figure S11), which is greatly enhanced compared to that (∼20%) in air. This demosntrates that the photooxiation is induced by oxygen.
(31) Zhang, L.; Zhou, Y.; Jia, M.; He, Y.; Hu, W.; Liu, Q.; Li, J.; Xu, X.; Wang, C.; Carlsson, A.; Lazar, S.; Meingast, A.; Ma, Y.; Xu, J.; Wen, W.; Liu, Z.; Cheng, J.; Deng, H. Covalent Organic Framework for Efficient Two-Photon Absorption. *Matter* **2020**, *2*, 1049−1063.
(32) Chen, C. X.; Yin, S. Y.; Wei, Z. W.; Qiu, Q. F.; Zhu, N. X.; Fan, Y. N.; Pan, M.; Su, C. Y. Pressure-Induced Multiphoton Excited Fluorochromic Metal-Organic Frameworks for Improving MPEF Properties. *Angew. Chem., Int. Ed.* **2019**, *58*, 14379−14385.
(33) Albota, M.; Beljonne, D.; Brédas, J.-L.; Ehrlich, J. E.; Fu, J.-Y.; Heikal, A. A.; Hess, S. E.; Kogej, T.; Levin, M. D.; Marder, S. R.; McCord-Maughon, D.; Perry, J. W.; Röckel, H.; Rumi, M.; Subramaniam, G.; Webb, W. W.; Wu, X.-L.; Xu, C. Design of Organic Molecules with Large Two-Photon Absorption Cross Sections. *Science* **1998**, *281*, 1653−1656.
(34) Zeng, J. Y.; Wang, X. S.; Xie, B. R.; Li, M. J.; Zhang, X. Z. Covalent Organic Framework for Improving Near-Infrared Light Induced Fluorescence Imaging through Two-Photon Induction. *Angew. Chem., Int. Ed.* **2020**, *59*, 10087−10094.
(35) Pascal, S.; David, S.; Andraud, C.; Maury, O. Near-infrared dyes for two-photon absorption in the short-wavelength infrared: strategies towards optical power limiting. *Chem. Soc. Rev.* **2021**, *50*, 6613−6658.
(36) Xu, L.; Zhang, J.; Yin, L.; Long, X.; Zhang, W.; Zhang, Q. Recent progress in efficient organic two-photon dyes for fluorescence imaging and photodynamic therapy. *J. Mater. Chem. C* **2020**, *8*, 6342−6349.




https://doi.org/10.1021/jacs.3c01517
*J. Am. Chem. Soc.* 2023, 145, 9771−9776